Biomolecules & Biomedicine

Biomolecules and Biomedicine
ISSN: 2831-0896 (Print) | ISSN: 2831-090X (Online)

Journal Impact Factor® (2022): 3.4
CiteScore® (2022): 5.3
www.biomolbiomed.com | blog.biomolbiomed.com

Rab8a/SNARE complex activation promotes vesicle anchoring and transport in spinal astrocytes to drive neuropathic pain

Yunqiao Xiao[1,2#], Gengyi Wang[1#], Guiqiong He[1], Wanxiang Qin[3], Ying Shi[4*]

[1]Institute of Neuroscience, Chongqing Medical University, Chongqing, China

[2]University-town hospital of Chongqing medical University, Chongqing, China

[3]Department of Pain Care, Southwest hospital, Army Medical University, Chongqing, China

[4]Department of Pain Care, The First Affiliated Hospital of Chongqing Medical University, Chongqing, China

[#]These authors contributed equally to this work.

[*]**Corresponding author:** Ying Shi; E-mail: driris56789@163.com

DOI: https://doi.org/10.17305/bb.2024.10441

Submitted: 06 March 2024/ **Accepted:** 23 April 2024/ **Published online:** 30 April 2024

Conflicts of interest: Authors declare no conflicts of interest.

Funding: This study was supported by Natural Science Foundation of Chongqing (cstc2019jcyj-msxmX0542) and Chongqing Science and Health Joint Medical Research Project (2021MSXM130).

Data availability: Data will be made available on request.

ABSTRACT

Neuropathic pain (NPP) remains a clinically challenging condition, driven by the activation of spinal astrocytes and the complex release of inflammatory mediators. This study aimed to examine the roles of Rab8a and SNARE complex proteins in activated astrocytes to uncover the underlying mechanisms of NPP. The research was conducted using a rat model with chronic constriction injury (CCI) of the sciatic nerve and primary astrocytes treated with lipopolysaccharide. Enhanced expression of Rab8a was noted specifically in spinal dorsal horn astrocytes through immunofluorescence. Electron microscopy observations showed increased vesicular transport and exocytic activity in activated astrocytes, which was corroborated by elevated levels of inflammatory cytokines such as IL-1β and TNF-α detected through quantitative PCR. Western blot analyses confirmed significant upregulation of Rab8a, VAMP2, and Syntaxin16 in these cells. Furthermore, the application of botulinum neurotoxin type A (BONT/A) reduced the levels of vesicle transport-associated proteins, inhibiting vesicular transport in activated astrocytes. These findings suggest that the Rab8a/SNARE pathway in astrocytes enhances vesicle transport and anchoring, increasing the secretion of bioactive molecules that may play a crucial role in the pathophysiology of NPP. Inhibiting this pathway with BONT/A offers a novel therapeutic target for managing NPP, highlighting its potential utility in clinical interventions.

KEYWORDS: Neuropathic pain, astrocytes, Rab8a, vesicular transport, SNARE proteins

INTRODUCTION

Neuropathic pain (NPP) represents a global therapeutic challenge characterized by complex pathophysiological mechanisms and a lack of effective clinical analgesics [1, 2, 3, 4, 5]. The functional specificity of cortical networks and their projection targets in the pain process occurs at least on four interconnected levels: dynamic activity states within the cortical network; functionally distinct subdomains; specific circuit connections that distinguish pain from other functions; and co-active cell assemblies [6]. Among these, intercellular communication and molecular signaling pathways within specific circuit connections play a pivotal role in the sensitization and regulation of nociceptive pathways in the sensory nervous system and the pathological process of NPP [7, 8, 9, 10].

Astrocytes, distinguishable by their expression of glial fibrillary acidic protein (GFAP) across all major branches and processes, dynamically modulate in response to injury through gap junction protein complexes that physically couple adjacent cells, allowing free exchange of ions and cytoplasmic components [11]. Inhibition of astrocyte activation can significantly alleviate pain caused by peripheral nerve damage in the early stages of NPP [12, 13, 14]. Astrocytes mediate intercellular communication within the nervous system through the production and secretion of neuroactive substances [15, 16, 17]. Injury signals drive phenotypic transformation of astrocytes and the release of inflammatory mediators, playing roles in central and peripheral sensitization and participating in the progression of NPP. An important characteristic of their activation is the increased release of bioactive molecules such as inflammatory factors, ATP, and glutamate [18, 19, 20, 21, 22, 23, 24].

Furthermore, astrocytes contain vesicles that store and release bioactive molecules in an activity-dependent manner, a principal mechanism in the pathophysiology of neurodegenerative diseases [25, 26, 27, 28, 29, 30, 31]. However, the specific mechanisms by which astrocytes in NPP increase the secretion of bioactive molecules remain unclear [32],

complicating the identification of targets for intervention.

Rab proteins, acting as molecular switches in vesicle transport, interact with upstream regulators and downstream effectors, playing a critical role in vesicle movement, docking, and fusion [33, 34]. In their active GTP-bound form, Rab proteins activate downstream effector proteins, recruit cytoplasmic adhesion factors, and regulate vesicle dynamics [35, 36, 37, 38, 39, 40, 41, 42]. The fusion of vesicles with the cell membrane also relies on a set of transmembrane proteins known as the SNARE complex, which provides the molecular basis for directed vesicle transport, targeting, docking, and membrane fusion [43, 44, 45]. Currently, the role of Rab8a in vesicle release processes in spinal astrocytes has not been reported. Thus, this study aims to examine the modification of Rab8a in activated astrocytes using a rat model with sciatic nerve ligation and lipopolysaccharide (LPS)-treated primary astrocytes to investigate its role in SNARE complex formation and vesicle transport and to explore the impact of the Rab8a/SNARE signaling pathway on NPP and its mechanisms. By revealing the role of this signaling pathway in regulating astrocyte vesicle transport and secretion functions, we aim to provide a new perspective on the molecular mechanisms of NPP and lay the groundwork for developing targeted therapeutic strategies, which hold significant scientific and clinical relevance.

MATERIALS AND METHODS

Experimental animals

Male Sprague-Dawley (SD) rats, aged 7-8 weeks (200-230 g), were obtained from the Experimental Animal Research Institute of the Army Medical University. These rats were housed in a controlled environment at 25°C with a 12-hour light/dark cycle, with free access to food and water. The animal experimental processes were approved by the Ethnic Committee of The First Affiliated Hospital of Chongqing Medical University

(AMUWEC20210719) and conducted in strict accordance with the standard of the Guide for the Care and Use of Laboratory Animals published by the Ministry of Science and Technology of the People's Republic of China in 2006.

Induction of NPP through chronic constriction injury (CCI)

Ten SD rats (aged 7-8 weeks, weighing 200-230 g) were utilized. The sample size calculation was based on setting the range of acceptable degrees of freedom (DF) for ANOVA analysis between 10 and 20. Let N represent the total number of subjects, k the number of groups, and n the number of subjects per group, calculated as $n = DF/k + 1$. Hence, the minimum total sample size N(min) was determined to be 6, and the maximum total sample size N(max) was 11 [46]. The ten rats were randomly divided into two groups: a normal group (control group, n=5) and a CCI group (ligation group, n=5). Each group underwent specific procedures: the normal group received a sham operation without ligation; the CCI group was subjected to a procedure established in previous studies [47]. Briefly, a blunt dissection was performed in the biceps femoris, exposing the common sciatic nerve at the mid-thigh level. Approximately 1 cm of the nerve was freed from surrounding connective tissue near its trifurcation, and three loops of 4.0 non-absorbable surgical suture (Shanghai Fosun) were loosely tied around it at 1 mm intervals. Under 30x magnification, these ties did not significantly compress the nerve's diameter but did induce slight and transient twitches in the muscles innervated by the sciatic nerve. The test animals were subsequently maintained for 14 days.

Astrocyte culture

Primary astrocytes were prepared from one-day-old SD rats, following the procedure described by Sebastian Schildge et al. [48]. These cells were isolated from the cerebral cortex and subsequently cultured in 25 cm^2 flasks pre-coated with 50 μg/mL poly-D-lysine. The

118 culture medium used was DMEM (Gibco, New York, USA) supplemented with 10%
119 heat-inactivated fetal bovine serum and 1% penicillin-streptomycin (Beyotime, Shanghai,
120 China). The cultures were maintained under conditions of 5% CO_2 at 37°C. The medium was
121 replaced the day following the initial culture and thereafter every two days. On the seventh
122 day, the cultures were placed on a rotating shaker at 37°C for 6 hours (240 rpm) to detach
123 microglial and oligodendrocyte precursor cells. Following this, the medium was discarded,
124 and the astrocytes were cultured at a final density of 1.2×10^6 cells per well in 6-well plates
125 and 4×10^4 cells per well in 96-well plates for subsequent cell counting kit-8 (CCK8) assay.
126 In the drug treatment groups, astrocytes were co-incubated with LPS (100 ng/mL) and
127 botulinum toxin A (BONT/A) (0.1 U/mL) for one hour [49, 50, 51, 52]. In this study, LPS
128 was used as a cell activator and BONT/A as a vesicular secretion inhibitor.
129 Immunofluorescence (IF) staining with GFAP (an astrocyte marker, BM-0055, Bioss, Wuhan,
130 China) was performed to identify the astrocytes. A high-purity population of astrocytes (over
131 95% GFAP-positive) was obtained [53]. To ensure cell culture quality, high-quality fetal
132 bovine serum and culture medium, along with sterile plastic products designed specifically
133 for tissue culture, were used. To prevent microbial contamination, 100 U/mL
134 penicillin-streptomycin (Bi Yun Tian, C0222) was employed to protect against cellular
135 contamination. Mycoplasma testing was performed prior to experiments to exclude
136 mycoplasma infections.
137
138 **Cell viability assay**
139 Cell viability was assessed using CCK-8 (Bioss, Beijing, China). Astrocytes were cultured in
140 96-well plates for 24 hours. Following treatment with LPS (100 ng/mL) for 24 hours, CCK-8
141 solution was added to each well and incubated at 37°C for 2 hours. Absorbance was
142 measured at 450 nm using a microplate reader.

143 **Immunohistochemistry (IHC)**

144 Spinal cord tissues from CCI rats were collected on day 14 post-sciatic nerve ligation. Rats
145 were deeply anesthetized with isoflurane (2-2.5%, airflow 500-700 mL/min) and then
146 perfused intracardially with 4% paraformaldehyde (Sigma) pre-cooled to 4°C. The spinal
147 cord was quickly removed and immersed in 4% paraformaldehyde at 4°C overnight. After
148 fixation, the spinal cord was dehydrated, and the lumbar enlargement region was sectioned
149 into 16 μm thick slices. Endogenous peroxidase activity was blocked using 3% H_2O_2 for 20
150 minutes. Sections were incubated with 10% normal goat serum and anti-Rab8a antibody
151 (1:150; LifeSpan Biosciences) at 37°C for 1 hour, followed by overnight incubation at 4°C.
152 After PBS rinsing, sections were incubated at 37°C for 1 hour and visualized using an
153 enhanced nickel-DAB staining reagent for 5 minutes. IHC images were captured using a
154 microscope (Leica). Five random spinal cord sections were selected by two experienced
155 pathologists in a blinded manner, and the average optical density of all positively stained
156 astrocytes in the selected fields was measured and analyzed using Image-Pro Plus 6.0.

157

158 **Immunofluorescence (IF) staining**

159 For double-labeling IF experiments on spinal cord sections, prepared slices were treated with
160 3% H_2O_2 for 20 minutes to suppress endogenous peroxidase activity. The sections were then
161 incubated at 37°C for 1 hour, followed by overnight treatment at 4°C with 10% normal goat
162 serum. Subsequently, the slices were incubated with anti-GFAP monoclonal antibody (1:250,
163 Bioss) at 37°C for 1 hour, followed by co-incubation with anti-Rab8a polyclonal antibody
164 (1:150, LifeSpan Biosciences) at 37°C for 1 hour, and then overnight at 4°C.
165 FITC-conjugated goat anti-mouse antibody (1:500, Abcam, UK) and Cy3-conjugated goat
166 anti-rabbit antibody (1:600, Jackson ImmunoResearch, USA) were added and incubated at
167 37°C for 1 hour. Finally, nuclei were stained with 4',6-diamidino-2-phenylindole (DAPI)

168 (Sigma, USA) and analyzed by two experienced pathologists in a blinded manner using a
169 laser scanning confocal microscope (Olympus, Japan).
170 For IF staining experiments detecting GFAP in astrocytes, astrocytes grown on microscope
171 slides were fixed in 4% paraformaldehyde at 37°C for 30 minutes, followed by incubation in
172 5% BSA at 37°C for 1 hour and then overnight incubated with anti-GFAP monoclonal
173 antibody (1:250, Bioss) at 4°C. The cells were then incubated at 37°C for 1 hour with
174 FITC-conjugated goat anti-mouse antibody (1:500, Abcam, UK). Nuclei were visualized with
175 DAPI staining (Bioss, Beijing, China), and images were captured using a microscope (Leica).
176 In the double-labeling, IF experiments, astrocytes grown on microscope slides were fixed
177 with 4% paraformaldehyde at 37°C for 30 minutes, then incubated in 5% BSA at 37°C for 1
178 hour, followed by overnight incubation with anti-Rab8a polyclonal antibody (1:250, LifeSpan
179 Biosciences) at 4°C. FITC-conjugated goat anti-mouse antibody (1:500, Abcam, UK) and
180 Cy3-conjugated goat anti-rabbit antibody (1:600, Jackson ImmunoResearch, USA) were
181 added and incubated at 37°C for 1 hour. Nuclei were stained with DAPI (Cat# D9542-5MG,
182 Sigma, USA) and analyzed using a laser scanning confocal microscope (Leica).
183
184 **Western blot assay**
185 Cell lysates were collected from primary astrocyte cultures in RIPA buffer containing a
186 protease inhibitor cocktail for Western blot analysis 1-hour post-LPS stimulation. The
187 reaction mixtures were centrifuged at 12,000 × g for 15 minutes at 4°C. Samples containing 2
188 μg of protein were heated at 100°C for 5 minutes in a loading buffer (5x Loading Buffer,
189 Beyotime, Shanghai, China). Separation was conducted using polyacrylamide gels (10-12.5%,
190 Epizyme, Beijing, China). Following membrane transfer, the membranes were incubated
191 overnight at 4°C with anti-GFAP monoclonal antibody (1:1000, Bioss), anti-Rab8a
192 polyclonal antibody (1:1000, LifeSpan), anti-VAMP2 polyclonal antibody (1:1000, Cell

193 Signaling), anti-Syntaxin16 polyclonal antibody (1:1000, Cell Signaling), and anti-β-actin
194 (1:1000, Proteintech). The membranes were then incubated for 1 hour with horseradish
195 peroxidase-conjugated secondary antibodies and visualized using ECL solution (Biosharp,
196 Shanghai, China). Immunocomplexes were detected using the Bio-Rad system, and relative
197 immunoreactivity levels were quantified using Image Lab software.
198
199 **Quantitative real-time polymerase chain reaction (qPCR)**
200 Total RNA from astrocytes was isolated using the RNAeasy™ animal RNA isolation kit with
201 the spin column, following the manufacturer's instructions (Beyotime, Shanghai, China).
202 RNA sample transcription was repeated using the PrimeScript™ RT reagent kit with gDNA
203 Eraser (Takara, Japan), according to the manufacturer's instructions. Real-time qPCR was
204 conducted using SYBR Premix Ex Taq II (Takara). The thermal cycling program included a
205 10-minute pre-incubation at 95°C, followed by 45 cycles of 10 seconds at 95°C, 30 seconds
206 at 60°C, and 60 seconds at 65°C. The specificity of the PCR products was verified through
207 melt curve analysis.
208
209 **Electron microscopy (EM)**
210 Astrocytes were co-incubated with LPS (100 ng/mL) or LPS (100 ng/mL) and BONT/A (0.1
211 U/mL) for 24 hours. Cells were then detached using a 0.025% trypsin-EDTA solution and
212 fixed with 2.5% glutaraldehyde at 4°C for 12 hours. The prepared cells were further fixed
213 with 1% osmium tetroxide at 4°C for 1 hour. After gradient dehydration, the cells were
214 embedded in resin. Embedded cell sections were then observed under a transmission EM.
215
216 **Ethical statement**
217 The animal experimental processes were approved by the Ethnic Committee of The First

218 Affiliated Hospital of Chongqing Medical University (AMUWEC20210719) and conducted
219 in strict accordance with the standard of the Guide for the Care and Use of Laboratory
220 Animals published by the Ministry of Science and Technology of the People's Republic of
221 China in 2006.
222
223 **Statistical analysis**
224 All statistical analyses were conducted using version 4.2.1 of R (R Foundation for Statistical
225 Computing). Quantitative data in this study were analyzed using GraphPad Prism version
226 9.5.0. Data were presented as mean ± standard deviation. Initially, tests for normality and
227 homogeneity of variance were performed. If the data were normally distributed and the
228 variances were homogeneous, unpaired t-tests were used to compare differences between two
229 groups. One-way analysis of variance (ANOVA) was employed to compare differences
230 among multiple groups, followed by Tukey's post-hoc test for pairwise comparisons. A $P <$
231 0.05 was considered statistically significant, while a $P < 0.01$ was considered highly
232 significant.
233
234 **RESULTS**
235 **Activation of astrocytes and increased Rab8a expression in the spinal dorsal horn of**
236 **CCI rats**
237 In our study of the sciatic nerve ligation model in rats, we conducted IHC and IF staining to
238 investigate the potential mechanisms related to astrocytes in NPP. IHC analysis revealed a
239 significant increase in Rab8a expression in the spinal dorsal horn of rats subjected to sciatic
240 nerve ligation compared to controls (Figure 1A-B, $P < 0.01$).
241 IF staining further explored the distribution of Rab8a in the spinal dorsal horn. GFAP (green
242 fluorescence), a marker of astrocytes, showed a notable increase in the NPP model, indicating

243 the activation of astrocytes. Rab8a (red fluorescence) staining was observed in various cell
244 types within the spinal dorsal horn, but a significant increase in Rab8a expression was
245 evident in activated astrocytes (Figure 1C). These findings highlight the association between
246 Rab8a expression and astrocyte activation, suggesting its potential importance in the
247 pathophysiology of NPP.
248
249 **Upregulation of cytokine expression in LPS-induced activated astrocytes**
250 LPS is commonly utilized to simulate inflammatory responses, prompting a series of
251 experiments to investigate its effects on astrocytes. Initially, we assessed the viability of
252 astrocytes to gauge the activating effect of LPS. The results demonstrated a significant
253 increase in the survival rate of astrocytes cultured with LPS compared to the control group
254 (Figure 2A, $P < 0.05$).
255 IF and Western blot analyses revealed a significant increase in the expression of the GFAP
256 protein in cells treated with LPS (Figure 2B, $P < 0.05$). Moreover, compared to the control
257 group, cells in the LPS group exhibited increased cell volume and shorter, thicker processes
258 (Figure 2C). This phenomenon likely reflects the morphological changes of astrocytes under
259 LPS treatment, further supporting their activated state.
260 Further analysis through qPCR was conducted to measure the mRNA levels of
261 pro-inflammatory cytokines, including TNF-α and IL-1β, in activated astrocytes. The results
262 showed significant upregulation of TNF-α and IL-1β mRNA levels in activated astrocytes
263 (Figure 3A-B, $P < 0.001$).
264 In summary, our findings reveal the activating effects of LPS on astrocytes, including
265 increased cell viability, elevated expression of GFAP protein, morphological changes, and the
266 upregulation of pro-inflammatory cytokines TNF-α and IL-1β mRNA levels in activated
267 astrocytes.

268 **Increased vesicular transport in LPS-induced activated astrocytes**

269 To investigate changes in vesicular transport within activated astrocytes, EM was employed
270 to examine vesicular transport. In the LPS-treated group, the Golgi apparatus was increased
271 and enlarged, with more Golgi vesicles around the trans-Golgi network (TGN).
272 Mitochondrial numbers were increased, showing swollen, spherical forms with reduced
273 cristae. The quantity of vesicles in activated astrocytes was higher in the LPS group, with
274 vesicles accumulating near the cell membrane (Figure 4A-B).

275 Given the molecular basis of vesicle and plasma membrane fusion established by the SNARE
276 complex [44], the co-expression of Rab8a and VAMP2 in activated astrocytes was further
277 investigated through IF experiments. It was observed that the positive IF staining of Rab8a
278 and VAMP2 was more aggregated in activated astrocytes. Additionally, astrocytes activated
279 by LPS also exhibited co-localization of Rab8a and VAMP2 expression, with these proteins
280 displaying a relatively uniform distribution across various cell types (Figure 5A).

281 Furthermore, co-localization of Rab8a and Syntaxin16 expression was also observed in
282 astrocytes activated by LPS. However, the distribution of the positive IF staining for Rab8a
283 and Syntaxin16 was not entirely consistent across different activated astrocytes (Figure 5B).

284 Western blot analysis further examined the expression levels of vesicular transport-related
285 proteins (Rab8a, VAMP2, and Syntaxin16). The results indicated that, following LPS
286 treatment, the levels of Rab8a, VAMP2, and Syntaxin16 proteins were significantly higher in
287 astrocytes compared to the control group (Figure 5C-E, $P < 0.05$).

288 These findings reveal increased vesicular transport in LPS-induced activated astrocytes,
289 accompanied by upregulation of protein levels of Rab8a and SNARE.

290

291 **BONT/A inhibits vesicular transport in LPS-induced activated astrocytes**

292 To assess the impact of the vesicular secretion inhibitor BONT/A on vesicular transport, we

293 conducted Western blot experiments to detect changes in proteins related to vesicular
294 transport (Rab8a, VAMP2, and Syntaxin16) in astrocytes activated by LPS treatment
295 following BONT/A administration. The results indicated a significant reduction in the
296 expression levels of Rab8a, VAMP2, and Syntaxin16 proteins in astrocytes treated with
297 BONT/A (BTX group) compared to those treated with LPS alone (LPS group) (Figure
298 6A-D).
299 To gain a comprehensive understanding of BONT/A's effect, EM was used to evaluate
300 changes in vesicular transport. The findings demonstrated that vesicular transport within
301 astrocytes activated by LPS was significantly inhibited following BONT/A treatment,
302 evidenced by a decrease in the number of intracellular vesicles and a marked reduction in
303 vesicle accumulation near the cell membrane (Figure 7A-B).
304 These results reveal the inhibitory effect of BONT/A on vesicular transport in astrocytes
305 activated by LPS induction.
306
307 **DISCUSSION**
308 Our research demonstrates that injury signals drive the transformation and activation of
309 astrocytes, leading to increased release of pain-associated bioactive molecules such as
310 inflammatory factors, ATP, and glutamate. These molecules play roles in central and
311 peripheral sensitization and contribute to the progression of NPP [18, 19]. Astrocyte
312 activation is a heterogeneous process involving multiple molecular, cellular, and functional
313 changes, including alterations in vesicular secretion [25, 54, 55, 56]. However, the specific
314 mechanisms underlying vesicle and inflammatory mediator release remain unclear [32].
315 Rab8a protein and the SNARE complex are involved in vesicle-directed transport, targeting
316 docking, and fusion with the cell membrane [43, 44, 45], but their mechanisms in NPP have
317 yet to be confirmed.

318 In our study using a CCI rat model, Rab8a was highly expressed in astrocytes within the
319 spinal dorsal horn following neural injury, suggesting increased vesicle docking and transport
320 activity, a possible manifestation of astrocyte activation. EM revealed a significant increase in
321 internal vesicle number and transport activity toward the plasma membrane, resulting in
322 heightened exocytic activity. Quantitative PCR, IF, and Western blot results showed
323 significant increases in the expression of cytokines such as TNF-α and IL-1β, as well as
324 Rab8a, VAMP2, and Syntaxin16 in activated astrocytes. Treatment with BONT/A
325 significantly reduced the levels of Rab8a, VAMP2, and Syntaxin16 proteins in astrocytes.
326 Collectively, these findings suggest that the activation of the Rab8a/SNARE complex
327 pathway is crucial for vesicular transport and bioactive molecule release in astrocytes and
328 represents an important component in the pathogenesis of NPP.
329 Rab8a, a small GTPase, is essential for vesicle transport in various cell types and is involved
330 in cilia formation [57, 58]. Rab8a can interact with effectors or directly with SNARE to
331 recognize t-SNARE on target membranes, promoting v-SNARE and t-SNARE pairing, thus
332 guiding vesicle-directed transport and targeted docking [59, 60, 61, 62, 63, 64]. The control
333 of vesicle transport by Rab8a may facilitate the formation of different membrane protrusions,
334 while VAMP2 and Syntaxin16, components of the SNARE complex, are critical proteins in
335 vesicle docking. Our results, combined with previous studies [65, 66], suggest that
336 Rab8a-mediated enhanced transport of vesicles from the trans-Golgi network (TGN) to the
337 plasma membrane may underpin the molecular basis for astrocyte release of bioactive
338 molecules involved in the onset and maintenance of NPP. Enhanced vesicular transport in
339 LPS-activated astrocyte models likely represents a crucial mechanism for the secretion of
340 bioactive molecules by activated astrocytes, with activated pathways for cytokine synthesis
341 and secretion contributing to disease progression.
342 Furthermore, the application of BONT/A suggests that targeting components of the SNARE

complex can effectively reduce vesicular transport in astrocytes. Preclinical and clinical studies have reported the efficacy of BONT/A in treating central NPP. BONT/A inhibits the secretion of substance P and CGRP in DRG, suppresses the expression of TRPV1 and P2X3, and exerts central effects through retrograde axonal transport [67, 68, 69, 70]. BONT/A not only cleaves SNAP-25 at presynaptic terminals but also cleaves SNARE proteins retrogradely in growth cones and the central brain, inhibiting the exocytosis of vesicles containing norepinephrine, glutamate, substance P, and calcitonin gene-related peptide (CGRP), as well as the expression of vanilloid receptors.

CONCLUSION

In summary, our study reveals that the activation of the Rab8a/SNARE complex pathway and subsequent enhanced vesicle transport activity in the spinal dorsal horn following neural injury are likely critical components in the cytokine cascade reaction mechanisms of NPP (Figure 8). By elucidating the role of the Rab8a/SNARE complex in the development of NPP, this study provides important insights for understanding the molecular basis of NPP and developing new therapeutic strategies. Given the persistent activation of astrocytes under chronic pain conditions and their recognized role in NPP, directing therapeutic interventions towards reactive astrocytes holds significant potential. Our research demonstrates the critical role of these proteins in astrocytes and emphasizes the importance of vesicle transport in regulating NPP, offering new potential targets for NPP treatment. Targeting the Rab8a/SNARE complex pathway could be an effective strategy for alleviating or treating NPP. Based on our current understanding of astrocyte-mediated NPP, considering targeting related signaling pathways, hemichannels, or purinergic receptors to inhibit the release of neuroglial mediators, such as by inhibiting the expression or function of Rab8a to reduce the release of inflammatory mediators, could provide valuable directions for developing novel

368 NPP therapeutic drugs. Additionally, targeting downstream mediators released by astrocytes,
369 such as chemokines and cytokine signaling, is a viable treatment strategy. Given that
370 astrocyte dysregulation is a common feature of nearly all chronic pain pathologies, and the
371 activation of astrocytes remains strong throughout persistent pain conditions, whether
372 targeting the activation of astrocytes or preventing their transition to a pro-inflammatory state
373 without affecting their normal homeostatic functions remains a significant challenge.
374 Although this study provides important insights into the role of the Rab8a/SNARE complex
375 in NPP, it has limitations. Firstly, the study is primarily based on animal models and cell
376 experiments, and its results need further validation in humans. Secondly, although BONT/A
377 can inhibit vesicular transport in astrocytes, its specific mechanisms of action and long-term
378 effects require further investigation. Additionally, this study did not fully resolve all potential
379 molecular mechanisms of the Rab8a/SNARE complex pathway in the pathogenesis of NPP,
380 necessitating further research to elucidate these mechanisms. Future research should focus on
381 several key areas. Firstly, the findings of this study need to be validated in a broader range of
382 biological models and explored through clinical studies to assess their potential application in
383 human NPP treatment. Secondly, specific intervention methods targeting the Rab8a/SNARE
384 complex pathway, including small molecule inhibitors, and RNA interference techniques,
385 should be explored to develop new treatment strategies. Additionally, investigating the role of
386 the Rab8a/SNARE complex in other cell types beyond astrocytes, such as neurons and
387 microglia, may reveal more complex pathological mechanisms of NPP.
388

389 **Author contributions**

390 YQX, GYW and YS designed the study. GQH and WXQ collated the data, carried out data
391 analyses and produced the initial draft of the manuscript. YQX, GYW and YS contributed to
392 drafting the manuscript. All authors have read and approved the final submitted manuscript.

393 **REFERENCES**

394 1. Garland E. L. (2014). Treating chronic pain: the need for non-opioid options. Expert
395 review of clinical pharmacology, 7(5), 545–550.
396 https://doi.org/10.1586/17512433.2014.928587

397 2. St John Smith E. (2018). Advances in understanding nociception and neuropathic pain.
398 Journal of neurology, 265(2), 231–238. https://doi.org/10.1007/s00415-017-8641-6

399 3. Moisset, X., Bouhassira, D., & Attal, N. (2021). French guidelines for neuropathic
400 pain: An update and commentary. Revue neurologique, 177(7), 834–837.
401 https://doi.org/10.1016/j.neurol.2021.07.004

402 4. Knotkova, H., Hamani, C., Sivanesan, E., Le Beuffe, M. F. E., Moon, J. Y., Cohen, S.
403 P., & Huntoon, M. A. (2021). Neuromodulation for chronic pain. Lancet (London, England),
404 397(10289), 2111–2124. https://doi.org/10.1016/S0140-6736(21)00794-7

405 5. Petzke, F., Tölle, T., Fitzcharles, M. A., & Häuser, W. (2022). Cannabis-Based
406 Medicines and Medical Cannabis for Chronic Neuropathic Pain. CNS drugs, 36(1), 31–44.
407 https://doi.org/10.1007/s40263-021-00879-w

408 6. Tan, L. L., & Kuner, R. (2021). Neocortical circuits in pain and pain relief. Nature
409 reviews. Neuroscience, 22(8), 458–471. https://doi.org/10.1038/s41583-021-00468-2

410 7. Burda, J. E., Bernstein, A. M., & Sofroniew, M. V. (2016). Astrocyte roles in traumatic
411 brain injury. Experimental neurology, 275 Pt 3(0 3), 305–315.
412 https://doi.org/10.1016/j.expneurol.2015.03.020

413 8. Okada, S., Hara, M., Kobayakawa, K., Matsumoto, Y., & Nakashima, Y. (2018).
414 Astrocyte reactivity and astrogliosis after spinal cord injury. Neuroscience research, 126, 39–
415 43. https://doi.org/10.1016/j.neures.2017.10.004

416 9. Goenaga, J., Araque, A., Kofuji, P., & Herrera Moro Chao, D. (2023). Calcium
417 signaling in astrocytes and gliotransmitter release. Frontiers in synaptic neuroscience, 15,

418 1138577. https://doi.org/10.3389/fnsyn.2023.1138577

419 10. Li, X., Jin, D. S., Eadara, S., Caterina, M. J., & Meffert, M. K. (2023). Regulation by
420 noncoding RNAs of local translation, injury responses, and pain in the peripheral nervous
421 system. Neurobiology of pain (Cambridge, Mass.), 13, 100119.
422 https://doi.org/10.1016/j.ynpai.2023.100119

423 11. Ji, R. R., Donnelly, C. R., & Nedergaard, M. (2019). Astrocytes in chronic pain and
424 itch. Nature reviews. Neuroscience, 20(11), 667–685.
425 https://doi.org/10.1038/s41583-019-0218-1

426 12. Ueda, H., Neyama, H., Nagai, J., Matsushita, Y., Tsukahara, T., & Tsukahara, R.
427 (2018). Involvement of lysophosphatidic acid-induced astrocyte activation underlying the
428 maintenance of partial sciatic nerve injury-induced neuropathic pain. Pain, 159(11), 2170–
429 2178. https://doi.org/10.1097/j.pain.0000000000001316

430 13. Dubový, P., Klusáková, I., Hradilová-Svíženská, I., Joukal, M., & Boadas-Vaello, P.
431 (2018). Activation of Astrocytes and Microglial Cells and CCL2/CCR2 Upregulation in the
432 Dorsolateral and Ventrolateral Nuclei of Periaqueductal Gray and Rostral Ventromedial
433 Medulla Following Different Types of Sciatic Nerve Injury. Frontiers in cellular neuroscience,
434 12, 40. https://doi.org/10.3389/fncel.2018.00040

435 14. Xie, K. Y., Wang, Q., Cao, D. J., Liu, J., & Xie, X. F. (2019). Spinal astrocytic
436 FGFR3 activation leads to mechanical hypersensitivity by increased TNF-α in spared nerve
437 injury. International journal of clinical and experimental pathology, 12(8), 2898–2908.

438 15. Wei, J., Su, W., Zhao, Y., Wei, Z., Hua, Y., Xue, P., Zhu, X., Chen, Y., & Chen, G.
439 (2022). Maresin 1 promotes nerve regeneration and alleviates neuropathic pain after nerve
440 injury. Journal of neuroinflammation, 19(1), 32. https://doi.org/10.1186/s12974-022-02405-1

441 16. Li, J., Tian, M., Hua, T., Wang, H., Yang, M., Li, W., Zhang, X., & Yuan, H. (2021).
442 Combination of autophagy and NFE2L2/NRF2 activation as a treatment approach for

443 neuropathic pain. Autophagy, 17(12), 4062–4082.
444 https://doi.org/10.1080/15548627.2021.1900498
445 17. Wang, K., Wang, S., Chen, Y., Wu, D., Hu, X., Lu, Y., Wang, L., Bao, L., Li, C., &
446 Zhang, X. (2021). Single-cell transcriptomic analysis of somatosensory neurons uncovers
447 temporal development of neuropathic pain. Cell research, 31(8), 904–918.
448 https://doi.org/10.1038/s41422-021-00479-9
449 18. Li, N. Q., Peng, Z., Xu, W. W., An, K., & Wan, L. (2021). Bone mesenchymal stem
450 cells attenuate resiniferatoxin-induced neuralgia via inhibiting
451 TRPA1-PKCδ-P38/MAPK-p-P65 pathway in mice. Brain research bulletin, 174, 92–102.
452 https://doi.org/10.1016/j.brainresbull.2021.06.004
453 19. Zhou, B., Zuo, Y. X., & Jiang, R. T. (2019). Astrocyte morphology: Diversity,
454 plasticity, and role in neurological diseases. CNS neuroscience & therapeutics, 25(6), 665–
455 673. https://doi.org/10.1111/cns.13123
456 20. Vay, S. U., Olschewski, D. N., Petereit, H., Lange, F., Nazarzadeh, N., Gross, E.,
457 Rabenstein, M., Blaschke, S. J., Fink, G. R., Schroeter, M., & Rueger, M. A. (2021).
458 Osteopontin regulates proliferation, migration, and survival of astrocytes depending on their
459 activation phenotype. Journal of neuroscience research, 99(11), 2822–2843.
460 https://doi.org/10.1002/jnr.24954
461 21. Falsig, J., Pörzgen, P., Lund, S., Schrattenholz, A., & Leist, M. (2006). The
462 inflammatory transcriptome of reactive murine astrocytes and implications for their innate
463 immune function. Journal of neurochemistry, 96(3), 893–907.
464 https://doi.org/10.1111/j.1471-4159.2005.03622.x
465 22. Ye, Y., Salvo, E., Romero-Reyes, M., Akerman, S., Shimizu, E., Kobayashi, Y.,
466 Michot, B., & Gibbs, J. (2021). Glia and Orofacial Pain: Progress and Future Directions.
467 International journal of molecular sciences, 22(10), 5345.

468 https://doi.org/10.3390/ijms22105345

469 23. Wang, H., & Xu, C. (2022). A Novel Progress: Glial Cells and Inflammatory Pain.
470 ACS chemical neuroscience, 13(3), 288–295. https://doi.org/10.1021/acschemneuro.1c00607

471 24. Higinio-Rodríguez, F., Rivera-Villaseñor, A., Calero-Vargas, I., & López-Hidalgo, M.
472 (2022). From nociception to pain perception, possible implications of astrocytes. Frontiers in
473 cellular neuroscience, 16, 972827. https://doi.org/10.3389/fncel.2022.972827

474 25. Sil, S., Singh, S., Chemparathy, D. T., Chivero, E. T., Gordon, L., & Buch, S. (2021).
475 Astrocytes & Astrocyte derived Extracellular Vesicles in Morphine Induced Amyloidopathy:
476 Implications for Cognitive Deficits in Opiate Abusers. Aging and disease, 12(6), 1389–1408.
477 https://doi.org/10.14336/AD.2021.0406

478 26. Datta Chaudhuri, A., Dasgheyb, R. M., DeVine, L. R., Bi, H., Cole, R. N., &
479 Haughey, N. J. (2020). Stimulus-dependent modifications in astrocyte-derived extracellular
480 vesicle cargo regulate neuronal excitability. Glia, 68(1), 128–144.
481 https://doi.org/10.1002/glia.23708

482 27. Frühbeis, C., Fröhlich, D., Kuo, W. P., Amphornrat, J., Thilemann, S., Saab, A. S.,
483 Kirchhoff, F., Möbius, W., Goebbels, S., Nave, K. A., Schneider, A., Simons, M., Klugmann,
484 M., Trotter, J., & Krämer-Albers, E. M. (2013). Neurotransmitter-triggered transfer of
485 exosomes mediates oligodendrocyte-neuron communication. PLoS biology, 11(7), e1001604.
486 https://doi.org/10.1371/journal.pbio.1001604

487 28. Upadhya, R., Zingg, W., Shetty, S., & Shetty, A. K. (2020). Astrocyte-derived
488 extracellular vesicles: Neuroreparative properties and role in the pathogenesis of
489 neurodegenerative disorders. Journal of controlled release : official journal of the Controlled
490 Release Society, 323, 225–239. https://doi.org/10.1016/j.jconrel.2020.04.017

491 29. Deng, Z., Wang, J., Xiao, Y., Li, F., Niu, L., Liu, X., Meng, L., & Zheng, H. (2021).
492 Ultrasound-mediated augmented exosome release from astrocytes alleviates

493 amyloid-β-induced neurotoxicity. Theranostics, 11(9), 4351–4362.
494 https://doi.org/10.7150/thno.52436
495 30. Liu, R., Wang, J., Chen, Y., Collier, J. M., Capuk, O., Jin, S., Sun, M., Mondal, S. K.,
496 Whiteside, T. L., Stolz, D. B., Yang, Y., & Begum, G. (2022). NOX activation in reactive
497 astrocytes regulates astrocytic LCN2 expression and neurodegeneration. Cell death & disease,
498 13(4), 371. https://doi.org/10.1038/s41419-022-04831-8
499 31. Abjean, L., Ben Haim, L., Riquelme-Perez, M., Gipchtein, P., Derbois, C., Palomares,
500 M. A., Petit, F., Hérard, A. S., Gaillard, M. C., Guillermier, M., Gaudin-Guérif, M., Aurégan,
501 G., Sagar, N., Héry, C., Dufour, N., Robil, N., Kabani, M., Melki, R., De la Grange, P.,
502 Bemelmans, A. P., … Escartin, C. (2023). Reactive astrocytes promote proteostasis in
503 Huntington's disease through the JAK2-STAT3 pathway. Brain : a journal of neurology,
504 146(1), 149–166. https://doi.org/10.1093/brain/awac068
505 32. Wang, M., Pan, W., Xu, Y., Zhang, J., Wan, J., & Jiang, H. (2022).
506 Microglia-Mediated Neuroinflammation: A Potential Target for the Treatment of
507 Cardiovascular Diseases. Journal of inflammation research, 15, 3083–3094.
508 https://doi.org/10.2147/JIR.S350109
509 33. Soldati, T., Shapiro, A. D., Svejstrup, A. B., & Pfeffer, S. R. (1994). Membrane
510 targeting of the small GTPase Rab9 is accompanied by nucleotide exchange. Nature,
511 369(6475), 76–78. https://doi.org/10.1038/369076a0
512 34. Langemeyer, L., Fröhlich, F., & Ungermann, C. (2018). Rab GTPase Function in
513 Endosome and Lysosome Biogenesis. Trends in cell biology, 28(11), 957–970.
514 https://doi.org/10.1016/j.tcb.2018.06.007
515 35. Hattula, K., Furuhjelm, J., Tikkanen, J., Tanhuanpää, K., Laakkonen, P., & Peränen, J.
516 (2006). Characterization of the Rab8-specific membrane traffic route linked to protrusion
517 formation. Journal of cell science, 119(Pt 23), 4866–4877. https://doi.org/10.1242/jcs.03275

518 36. Peränen J. (2011). Rab8 GTPase as a regulator of cell shape. Cytoskeleton (Hoboken,
519 N.J.), 68(10), 527–539. https://doi.org/10.1002/cm.20529
520 37. Vaibhava, V., Nagabhushana, A., Chalasani, M. L., Sudhakar, C., Kumari, A., &
521 Swarup, G. (2012). Optineurin mediates a negative regulation of Rab8 by the
522 GTPase-activating protein TBC1D17. Journal of cell science, 125(Pt 21), 5026–5039.
523 https://doi.org/10.1242/jcs.102327
524 38. Kim, M. J., Deng, H. X., Wong, Y. C., Siddique, T., & Krainc, D. (2017). The
525 Parkinson's disease-linked protein TMEM230 is required for Rab8a-mediated secretory
526 vesicle trafficking and retromer trafficking. Human molecular genetics, 26(4), 729–741.
527 https://doi.org/10.1093/hmg/ddw413
528 39. Grigoriev, I., Yu, K. L., Martinez-Sanchez, E., Serra-Marques, A., Smal, I., Meijering,
529 E., Demmers, J., Peränen, J., Pasterkamp, R. J., van der Sluijs, P., Hoogenraad, C. C., &
530 Akhmanova, A. (2011). Rab6, Rab8, and MICAL3 cooperate in controlling docking and
531 fusion of exocytotic carriers. Current biology : CB, 21(11), 967–974.
532 https://doi.org/10.1016/j.cub.2011.04.030
533 40. Zhao, Y. G., Codogno, P., & Zhang, H. (2021). Machinery, regulation and
534 pathophysiological implications of autophagosome maturation. Nature reviews. Molecular
535 cell biology, 22(11), 733–750. https://doi.org/10.1038/s41580-021-00392-4
536 41. Usmani, A., Shavarebi, F., & Hiniker, A. (2021). The Cell Biology of LRRK2 in
537 Parkinson's Disease. Molecular and cellular biology, 41(5), e00660-20.
538 https://doi.org/10.1128/MCB.00660-20
539 42. Moreno-Layseca, P., Jäntti, N. Z., Godbole, R., Sommer, C., Jacquemet, G.,
540 Al-Akhrass, H., Conway, J. R. W., Kronqvist, P., Kallionpää, R. E., Oliveira-Ferrer, L.,
541 Cervero, P., Linder, S., Aepfelbacher, M., Zauber, H., Rae, J., Parton, R. G., Disanza, A.,
542 Scita, G., Mayor, S., Selbach, M., … Ivaska, J. (2021). Cargo-specific recruitment in clathrin-

543 and dynamin-independent endocytosis. Nature cell biology, 23(10), 1073–1084.
544 https://doi.org/10.1038/s41556-021-00767-x
545 43. Sundaresan, S., Philosoph-Hadas, S., Riov, J., Salim, S., & Meir, S. (2020).
546 Expression Kinetics of Regulatory Genes Involved in the Vesicle Trafficking Processes
547 Operating in Tomato Flower Abscission Zone Cells during Pedicel Abscission. Life (Basel,
548 Switzerland), 10(11), 273. https://doi.org/10.3390/life10110273
549 44. Margiotta A. (2021). Role of SNAREs in Neurodegenerative Diseases. Cells, 10(5),
550 991. https://doi.org/10.3390/cells10050991
551 45. Cupertino, R. B., Kappel, D. B., Bandeira, C. E., Schuch, J. B., da Silva, B. S.,
552 Müller, D., Bau, C. H., & Mota, N. R. (2016). SNARE complex in developmental psychiatry:
553 neurotransmitter exocytosis and beyond. Journal of neural transmission (Vienna, Austria :
554 1996), 123(8), 867–883. https://doi.org/10.1007/s00702-016-1514-9
555 46. Cao Ce, Li Lingmei, Zi Mingjie, et al. Methods for Determining Sample Size in
556 Animal Experiments in Medical Research. Chinese Journal of Comparative Medicine, 2023,
557 33(2): 99-105. https://doi.org/10.3969/j.issn.1671-7856.2023.02.013
558 47. Charlson, M. E., Carrozzino, D., Guidi, J., & Patierno, C. (2022). Charlson
559 Comorbidity Index: A Critical Review of Clinimetric Properties. Psychotherapy and
560 psychosomatics, 91(1), 8–35. https://doi.org/10.1159/000521288
561 48. Schildge, S., Bohrer, C., Beck, K., & Schachtrup, C. (2013). Isolation and culture of
562 mouse cortical astrocytes. Journal of visualized experiments : JoVE, (71), 50079.
563 https://doi.org/10.3791/50079
564 49. Han, J., Cho, H. J., Park, D., & Han, S. (2022). DICAM in the Extracellular Vesicles
565 from Astrocytes Attenuates Microglia Activation and Neuroinflammation. Cells, 11(19), 2977.
566 https://doi.org/10.3390/cells11192977
567 50. Przanowski, P., Dabrowski, M., Ellert-Miklaszewska, A., Kloss, M., Mieczkowski, J.,

568 Kaza, B., Ronowicz, A., Hu, F., Piotrowski, A., Kettenmann, H., Komorowski, J., &
569 Kaminska, B. (2014). The signal transducers Stat1 and Stat3 and their novel target Jmjd3
570 drive the expression of inflammatory genes in microglia. Journal of molecular medicine
571 (Berlin, Germany), 92(3), 239–254. https://doi.org/10.1007/s00109-013-1090-5
572 51. Popiolek-Barczyk, K., Kolosowska, N., Piotrowska, A., Makuch, W., Rojewska, E.,
573 Jurga, A. M., Pilat, D., & Mika, J. (2015). Parthenolide Relieves Pain and Promotes M2
574 Microglia/Macrophage Polarization in Rat Model of Neuropathy. Neural plasticity, 2015,
575 676473. https://doi.org/10.1155/2015/676473
576 52. Piotrowska, A., Popiolek-Barczyk, K., Pavone, F., & Mika, J. (2017). Comparison of
577 the Expression Changes after Botulinum Toxin Type A and Minocycline Administration in
578 Lipopolysaccharide-Stimulated Rat Microglial and Astroglial Cultures. Frontiers in cellular
579 and infection microbiology, 7, 141. https://doi.org/10.3389/fcimb.2017.00141
580 53. Zawadzka, M., & Kaminska, B. (2005). A novel mechanism of FK506-mediated
581 neuroprotection: downregulation of cytokine expression in glial cells. Glia, 49(1), 36–51.
582 https://doi.org/10.1002/glia.20092
583 54. Rolls, A., Shechter, R., & Schwartz, M. (2009). The bright side of the glial scar in
584 CNS repair. Nature reviews. Neuroscience, 10(3), 235–241. https://doi.org/10.1038/nrn2591
585 55. Bal-Price, A., & Brown, G. C. (2001). Inflammatory neurodegeneration mediated by
586 nitric oxide from activated glia-inhibiting neuronal respiration, causing glutamate release and
587 excitotoxicity. The Journal of neuroscience : the official journal of the Society for
588 Neuroscience, 21(17), 6480–6491. https://doi.org/10.1523/JNEUROSCI.21-17-06480.2001
589 56. Linnerbauer, M., Wheeler, M. A., & Quintana, F. J. (2020). Astrocyte Crosstalk in
590 CNS Inflammation. Neuron, 108(4), 608–622. https://doi.org/10.1016/j.neuron.2020.08.012
591 57. Waschbüsch, D., Purlyte, E., & Khan, A. R. (2021). Dual arginine recognition of
592 LRRK2 phosphorylated Rab GTPases. Biophysical journal, 120(9), 1846–1855.

593 https://doi.org/10.1016/j.bpj.2021.03.030
594 58. Dhekne, H. S., Yanatori, I., Vides, E. G., Sobu, Y., Diez, F., Tonelli, F., & Pfeffer, S.
595 R. (2021). LRRK2-phosphorylated Rab10 sequesters Myosin Va with RILPL2 during
596 ciliogenesis blockade. Life science alliance, 4(5), e202101050.
597 https://doi.org/10.26508/lsa.202101050
598 59. Yoshimura, S., Egerer, J., Fuchs, E., Haas, A. K., & Barr, F. A. (2007). Functional
599 dissection of Rab GTPases involved in primary cilium formation. The Journal of cell biology,
600 178(3), 363–369. https://doi.org/10.1083/jcb.200703047
601 60. Nachury, M. V., Loktev, A. V., Zhang, Q., Westlake, C. J., Peränen, J., Merdes, A.,
602 Slusarski, D. C., Scheller, R. H., Bazan, J. F., Sheffield, V. C., & Jackson, P. K. (2007). A core
603 complex of BBS proteins cooperates with the GTPase Rab8 to promote ciliary membrane
604 biogenesis. Cell, 129(6), 1201–1213. https://doi.org/10.1016/j.cell.2007.03.053
605 61. Knödler, A., Feng, S., Zhang, J., Zhang, X., Das, A., Peränen, J., & Guo, W. (2010).
606 Coordination of Rab8 and Rab11 in primary ciliogenesis. Proceedings of the National
607 Academy of Sciences of the United States of America, 107(14), 6346–6351.
608 https://doi.org/10.1073/pnas.1002401107
609 62. Westlake, C. J., Baye, L. M., Nachury, M. V., Wright, K. J., Ervin, K. E., Phu, L.,
610 Chalouni, C., Beck, J. S., Kirkpatrick, D. S., Slusarski, D. C., Sheffield, V. C., Scheller, R. H.,
611 & Jackson, P. K. (2011). Primary cilia membrane assembly is initiated by Rab11 and
612 transport protein particle II (TRAPPII) complex-dependent trafficking of Rabin8 to the
613 centrosome. Proceedings of the National Academy of Sciences of the United States of
614 America, 108(7), 2759–2764. https://doi.org/10.1073/pnas.1018823108
615 63. Feng, S., Knödler, A., Ren, J., Zhang, J., Zhang, X., Hong, Y., Huang, S., Peränen, J.,
616 & Guo, W. (2012). A Rab8 guanine nucleotide exchange factor-effector interaction network
617 regulates primary ciliogenesis. The Journal of biological chemistry, 287(19), 15602–15609.

618 https://doi.org/10.1074/jbc.M111.333245

619 64. Lu, Q., Insinna, C., Ott, C., Stauffer, J., Pintado, P. A., Rahajeng, J., Baxa, U., Walia,
620 V., Cuenca, A., Hwang, Y. S., Daar, I. O., Lopes, S., Lippincott-Schwartz, J., Jackson, P. K.,
621 Caplan, S., & Westlake, C. J. (2015). Early steps in primary cilium assembly require
622 EHD1/EHD3-dependent ciliary vesicle formation. Nature cell biology, 17(3), 228–240.
623 https://doi.org/10.1038/ncb3109

624 65. Mirzahosseini, G., Ismael, S., Ahmed, H. A., & Ishrat, T. (2021). Manifestation of
625 renin angiotensin system modulation in traumatic brain injury. Metabolic brain disease, 36(6),
626 1079–1086. https://doi.org/10.1007/s11011-021-00728-1

627 66. Pinheiro Campos, A. C., Martinez, R. C. R., Auada, A. V. V., Lebrun, I., Fonoff, E. T.,
628 Hamani, C., & Pagano, R. L. (2022). Effect of Subthalamic Stimulation and Electrode
629 Implantation in the Striatal Microenvironment in a Parkinson's Disease Rat Model.
630 International journal of molecular sciences, 23(20), 12116.
631 https://doi.org/10.3390/ijms232012116

632 67. Brin, M. F., & Burstein, R. (2023). Botox (onabotulinumtoxinA) mechanism of
633 action. Medicine, 102(S1), e32372. https://doi.org/10.1097/MD.0000000000032372

634 68. Park, J., & Park, H. J. (2017). Botulinum Toxin for the Treatment of Neuropathic
635 Pain. Toxins, 9(9), 260. https://doi.org/10.3390/toxins9090260

636 69. Reyes-Long, S., Alfaro-Rodríguez, A., Cortes-Altamirano, J. L., Lara-Padilla, E.,
637 Herrera-Maria, E., Romero-Morelos, P., Salcedo, M., & Bandala, C. (2021). The Mechanisms
638 of Action of Botulinum Toxin Type A in Nociceptive and Neuropathic Pathways in Cancer
639 Pain. Current medicinal chemistry, 28(15), 2996–3009.
640 https://doi.org/10.2174/0929867327666200806105024

641 70. Li, X., Guo, R., Sun, Y., Li, H., Ma, D., Zhang, C., Guan, Y., Li, J., & Wang, Y.
642 (2018). Botulinum toxin type A and gabapentin attenuate postoperative pain and NK1

receptor internalization in rats. Neurochemistry international, 116, 52–62. https://doi.org/10.1016/j.neuint.2018.03.010

TABLES AND FIGURES WITH LEGENDS

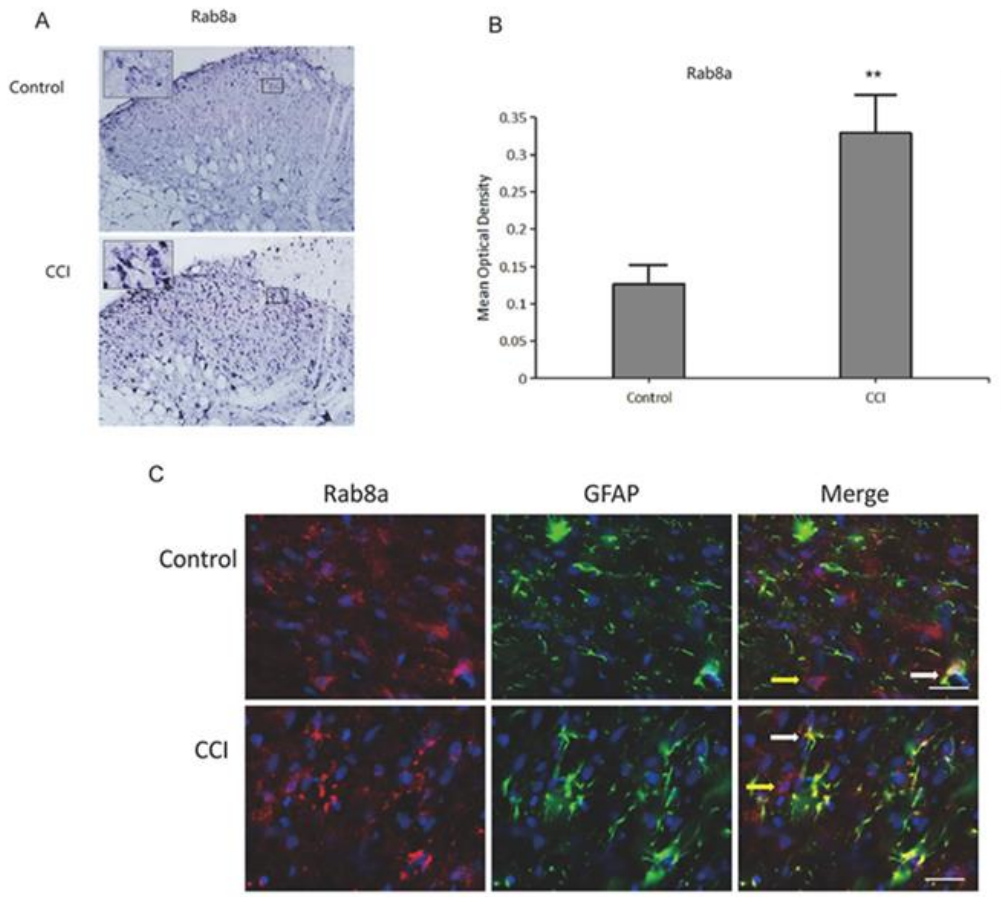

Figure 1. Activation of astrocytes and Rab8a expression in the spinal dorsal horn of CCI rats. (A) IHC staining of Rab8a in the spinal dorsal horn of CCI rats; (B) Quantitative analysis of Rab8a protein in the spinal dorsal horn of CCI rats; (C) IF staining in the spinal dorsal horn of CCI rats, showing GFAP-positive cells (green fluorescence) and the distribution of Rab8a (red fluorescence). $^{**}P < 0.01$. CCI: Chronic constriction injury; IHC: Immunohistochemistry; GFAP: Glial fibrillary acidic protein.

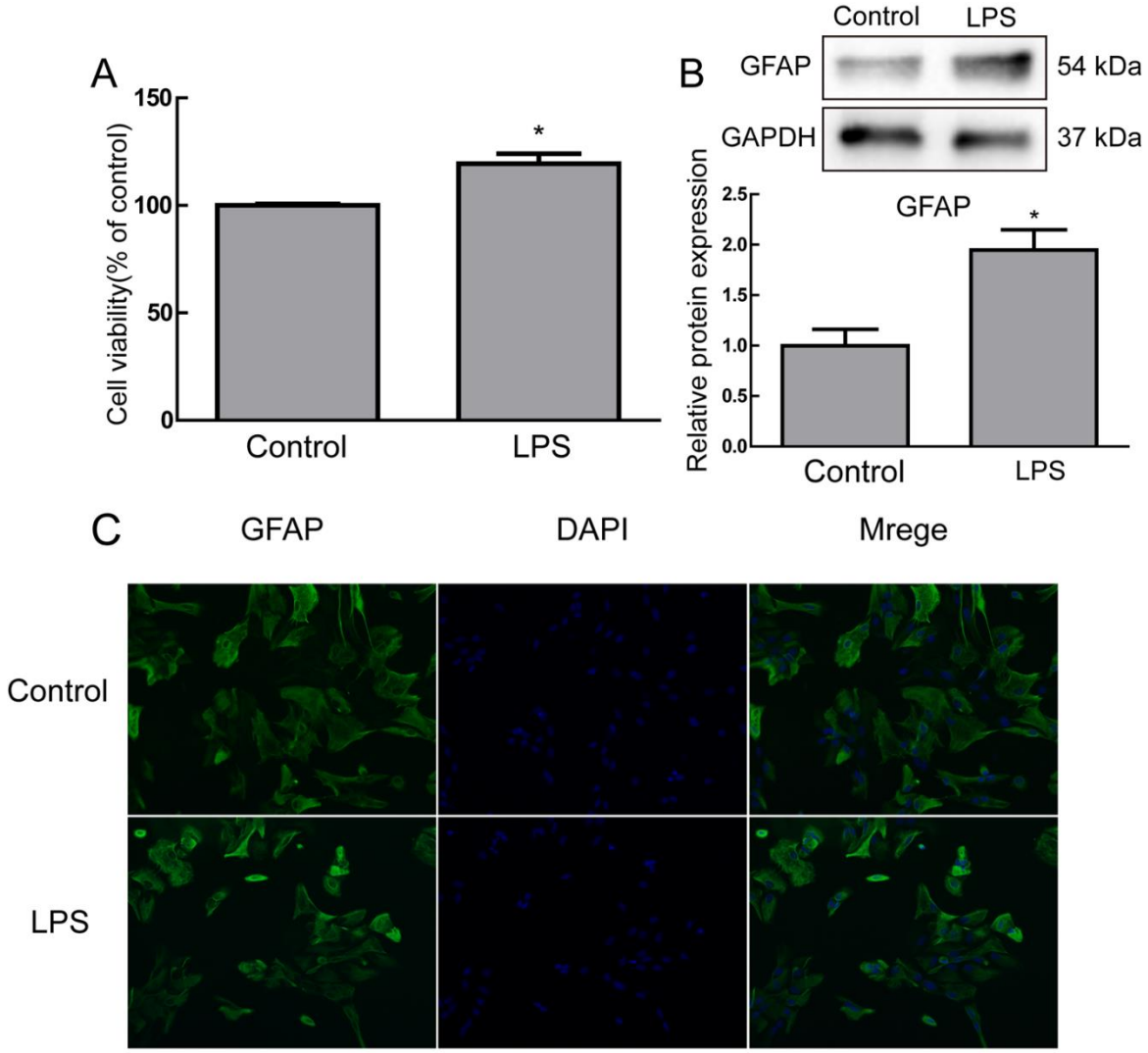

Figure 2. The effects of LPS on astrocytes. (A) The survival rate of astrocytes post-LPS treatment; (B) GFAP protein expression in astrocytes post-LPS treatment detected by Western blot; (C) IF staining of astrocytes post-LPS treatment, showing GFAP-positive cells (green fluorescence) and morphological changes. *$P < 0.05$. GFAP: Glial fibrillary acidic protein; LPS: Lipopolysaccharide; IF: Immunofluorescence.

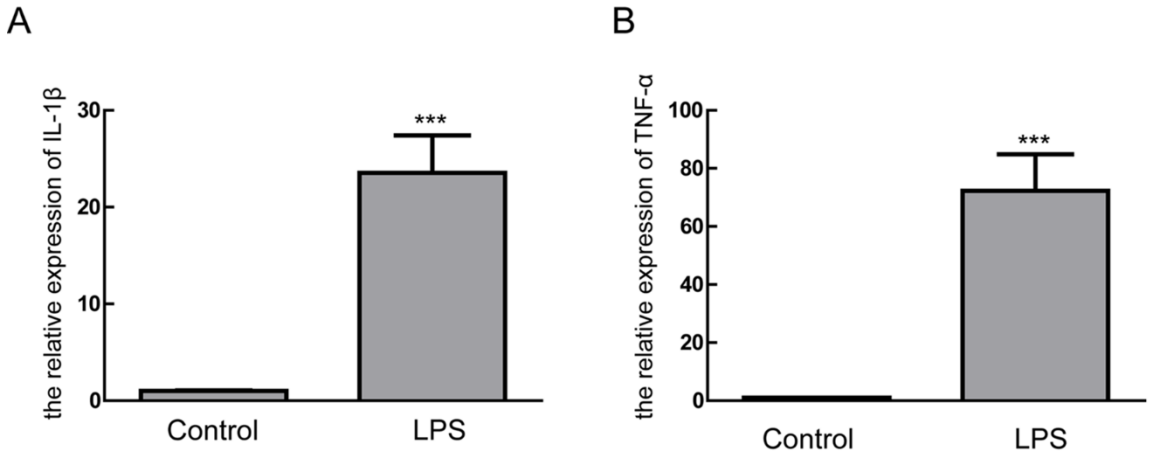

Figure 3. Expression of cytokines in activated astrocytes. (A) qPCR detection of TNF-α mRNA levels in astrocytes post-LPS treatment; (B) qPCR detection of IL-1β mRNA levels in astrocytes post-LPS treatment. ***$P < 0.001$. LPS: Lipopolysaccharide.

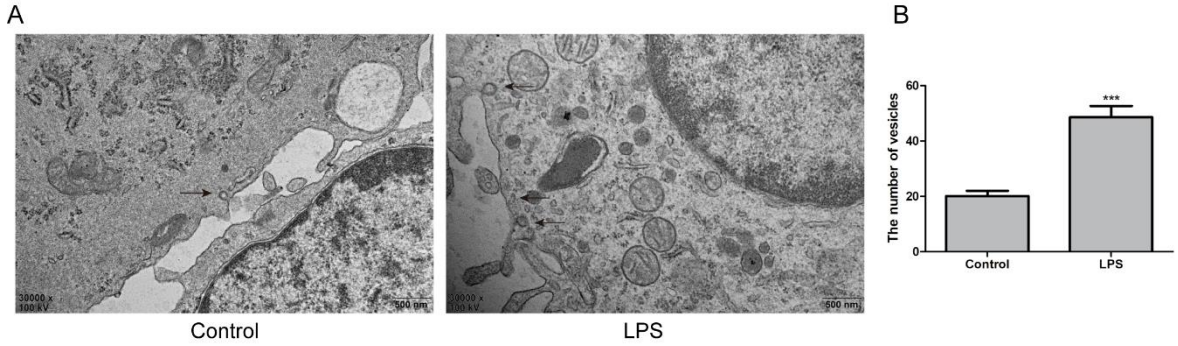

Figure 4. Changes in vesicular transport in activated astrocytes. (A) EM observation of vesicular transport in astrocytes post-LPS treatment; (B) Statistical graph of vesicular transport quantity in astrocytes post-LPS treatment. ***$P < 0.001$. EM: Electron microscopy; LPS: Lipopolysaccharide.

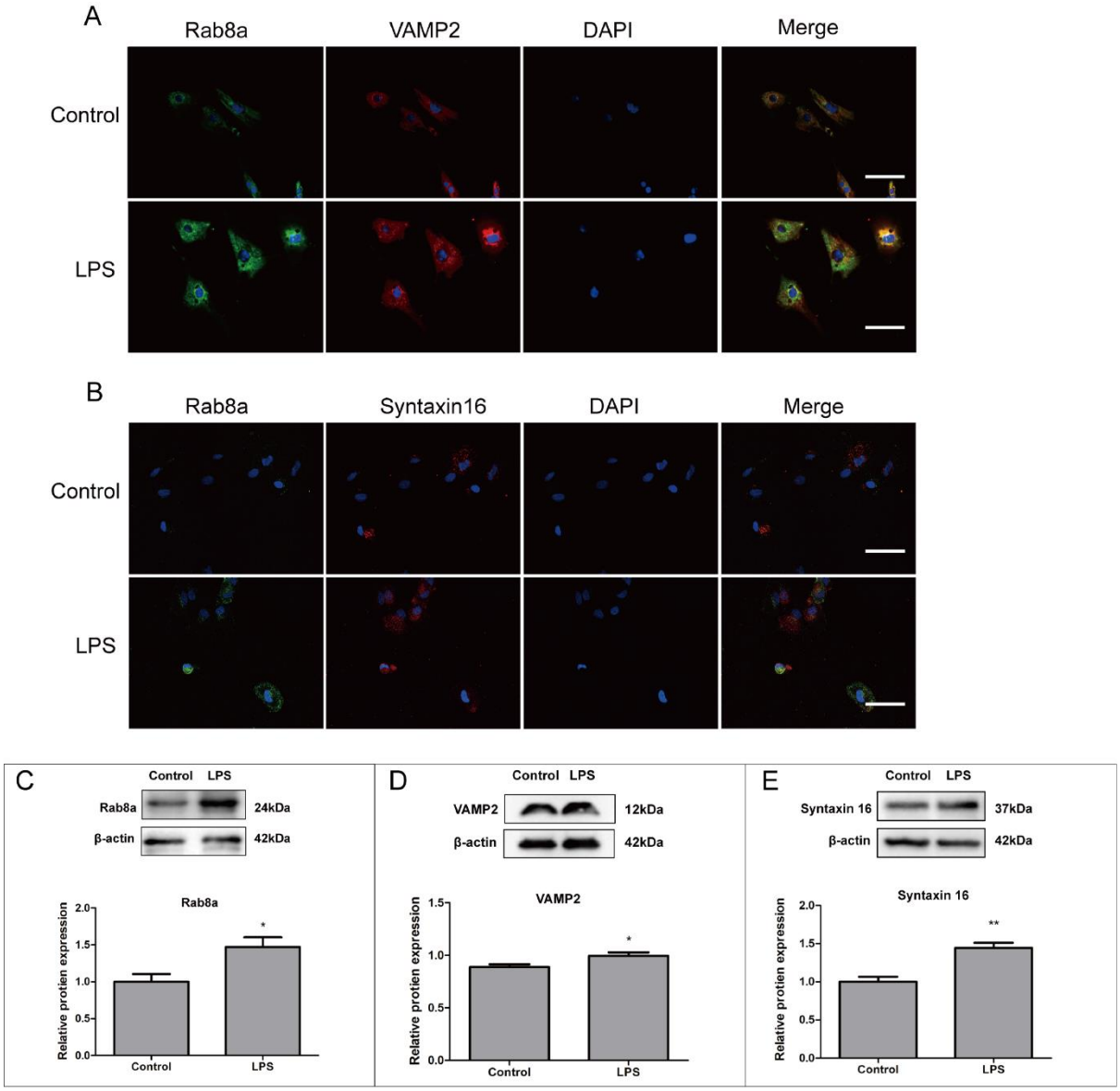

Figure 5. Levels of vesicular transport-related proteins in activated astrocytes. (A-B) IF staining of VAMP2 and Syntaxin16 in astrocytes post-LPS treatment; (C-E) Western blot detection of Rab8a and SNARE proteins (VAMP2 and Syntaxin16) levels in astrocytes post-LPS treatment. $*P < 0.05$, $**P < 0.01$. IF: Immunofluorescence; VAMP2: Vesicle-associated membrane protein; SNARE: Soluble N-ethylmaleimide-sensitive factor attachment protein receptor.

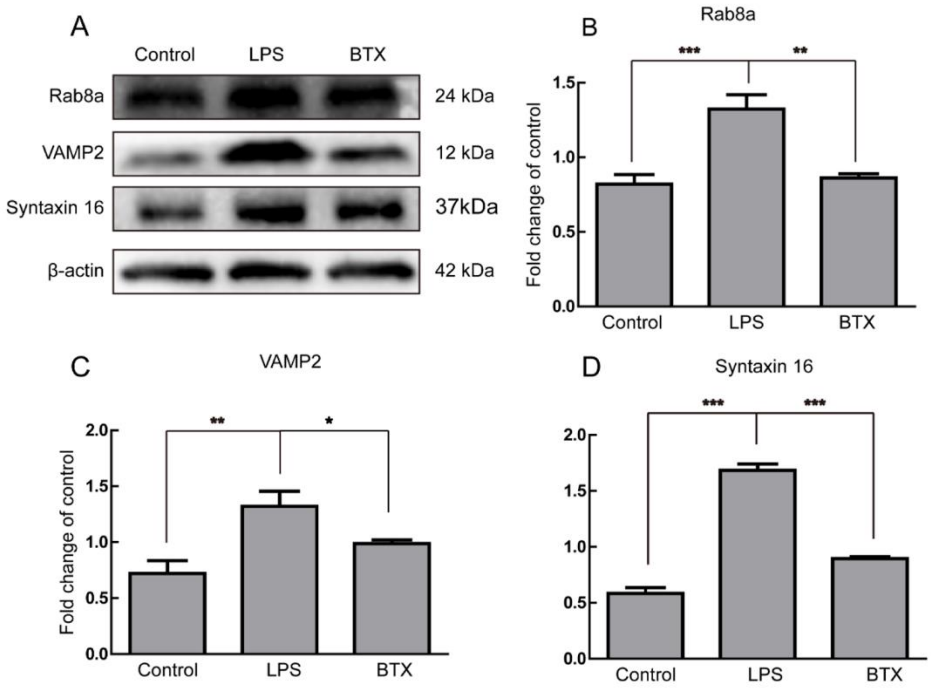

Figure 6. Effects of BONT/A on vesicular transport-related proteins in activated astrocytes. (A) Western blot detection of Rab8a, VAMP2, and Syntaxin16 protein expression in activated astrocytes post-BONT/A treatment; (B-D) Quantitative analysis of Rab8a, VAMP2, and Syntaxin16 proteins in activated astrocytes post-BONT/A treatment. *$P < 0.05$, **$P < 0.01$, ***$P < 0.001$. BONT/A: Botulinum neurotoxin type A.

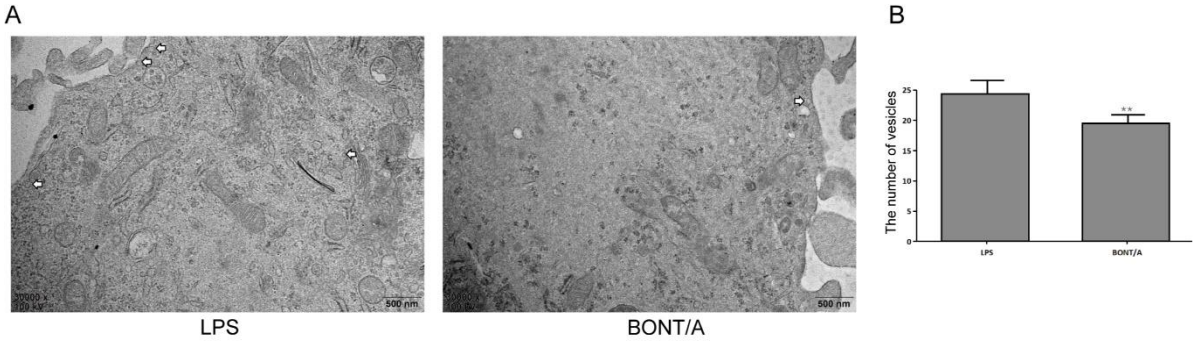

Figure 7. Effects of BONT/A on vesicular transport in activated astrocytes. (A) EM observation of vesicular transport in activated astrocytes post-BONT/A treatment; (B) Statistical analysis of vesicular transport quantity in activated astrocytes post-BONT/A treatment. **$P < 0.01$. BONT/A: Botulinum neurotoxin type A; EM: Electron microscopy.

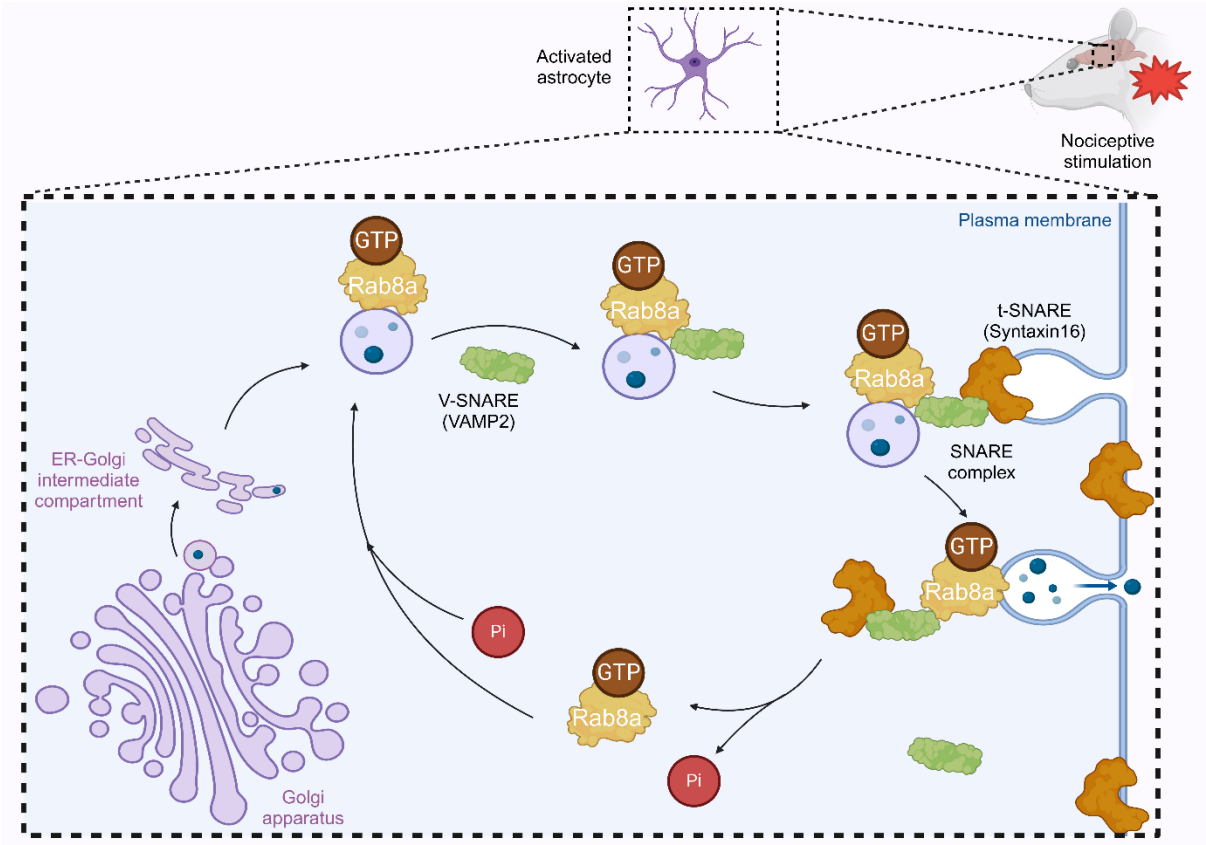

Figure 8. Activated Rab8a/SNARE complex drives the molecular mechanism of NPP by promoting vesicle anchoring and transportation in spinal astrocytes. NPP: Neuropathic pain.